Biochimica et Biophysica Acta 1827 (2013) 779–785

Contents lists available at SciVerse ScienceDirect

Biochimica et Biophysica Acta

journal homepage: www.elsevier.com/locate/bbabio

# Photochemical trapping heterogeneity as a function of wavelength, in plant photosystem I (PSI–LHCI)

Robert C. Jennings *, Giuseppe Zucchelli, Stefano Santabarbara

*Istituto di Biofisica, Consiglio Nazionale delle Ricerche, via Celoria 26, 20133 Milano, Italy*
*Dipartimento di Bioscienze, Università di Milano, via Celoria 26, 20133 Milano, Italy*

ARTICLE INFO

*Article history:*
Received 9 January 2013
Received in revised form 12 March 2013
Accepted 20 March 2013
Available online 28 March 2013

*Keywords:*
Photosystem I
Light Harvesting Complex I
Fluorescence decay
Trapping rate heterogeneity
Red spectral forms

ABSTRACT

In the present paper the marked changes in photochemical trapping time over the absorption/fluorescence band of isolated PSI–LHCI are studied by means of time resolved fluorescence decay measurements. For emission at 680–690 nm the effective trapping time is close to 17–18 ps, and represents the effective trapping time from the bulk antenna. At wavelengths above 700 nm the effective trapping time increases in a monotonic way, over the entire emission band, to attain values in the range of 70–80 ps near 760 nm. This is argued to be caused by "uphill" energy transfer from the low energy states to the core antenna and reaction centre. These data, together with the steady state emission spectrum, permit calculation of the overall trapping time for maize PSI–LHCI, which is estimated to be approximately 40 ps. The wavelength dependence of the trapping time indicates, that in PSI–LHCI there exists at least one red form which emits at lower energies than the 735 nm state. These data indicate that Photosystem I is about 55% diffusion limited.



## 1. Introduction

Photosystem I (PSI) of higher plants is a supramolecular pigment–protein complex, localized in the non-appressed regions of thylakoid membranes. The catalytic activity of PSI is that of a light-dependent oxido-reductase, which uses the diffusible electron carries plastocyanin as the electron donors and ferredoxin as the electron acceptors [1]. The complex has two functional moieties, which are the central chl *a*-binding core complex and a peripheral antenna, which consists of chlorophyll *a*/*b* binding proteins known collectively as LHCI. The core complex binds approximately 95 chl *a* and probably about 20 β-carotene molecules [2,3] as well as the cofactors involved in primary photochemical events and the successive electron transfer reactions. The LHCI complexes seem to be arranged on one side of the core [2,4] and, taken together, they bind about 66 chl *a* + *b* according to the crystallographic structure [2] and 80–100 according to biochemical analysis [5], and 20 xanthophylls, with the number of complexes surrounding the core probably being four according to the crystallographic structure and around 10 according to biochemical analysis [5]. The LHCI complexes are now thought to bind around 15–16 chlorophylls per monomer [2].

The PSI–LHCI supercomplex can be isolated from maize in an intact form, that is, without detergent-solubilized chls present [6]. In the region of the lowest lying electronic transition ($Q_y$), the complex has a broad absorption band with its maximum at 680 nm. This band is associated with the so-called "bulk" antenna chl *a* and accounts for about 90–95% of the $Q_y$ oscillator strength. A peculiarity of the PSI–LHCI absorption spectrum is the presence of significant absorption in the low-energy tail, indicating the presence of red spectral chl *a* forms, or states, absorbing at energies lower than that of the primary electron donor pigments from which photochemistry takes place, including the electron donor $P_{700}$. In PSI–LHCI the combined oscillator strength of the "red forms" is approximately equivalent to 7–8 chls [6] which, at room temperature, in the steady state, are highly populated, with 80–90% of the PSI–LHCI excited states being associated with them [6]. These low energy states have been demonstrated to be associated with excitonic dimers in the case of the cyanobacterium *Spirulina platensis* [7], in which the interaction energy was estimated to be 330–340 $cm^{-1}$, and also for the approximately 735 nm emission states in the external antenna complexes of PSI–LHCI [8,9]. It has been experimentally demonstrated that the red forms, located primarily in the peripheral antenna in plant PSI–LHCI [10–12], are kinetically limiting for the transfer of energy from the antenna to the reaction centre [13,14], indicating that PSI is partially diffusion limited, though there is some disagreement on this point [15].

The most widely used technique to study PSI–LHCI photochemical trapping involves measurement of the fluorescence lifetime decay, either by means of streak camera or of single photon counting techniques, which are subjected to global lifetime analysis. It is a common

*Abbreviations:* PSI, Photosystem I; LHC, Light Harvesting Complex; RC, reaction centre; DAS, decay associated spectra; SOI, spectral overlap integral; OGP, octyl-gluco-pyranoside; DM, dodecyl-maltoside

* Corresponding author at: Dipartimento di Bioscienze, Università di Milano, via Celoria 26, 20133 Milano, Italy. Tel.: +39 02 503 14858.
*E-mail address:* robert.jennings@unimi.it (R.C. Jennings).

0005-2728/$ – see front matter © 2013 Elsevier B.V. All rights reserved.
http://dx.doi.org/10.1016/j.bbabio.2013.03.008

practice to associate the trapping time to decay associated spectra (DAS) [e.g. 13–18] that display positive amplitude across the whole fluorescence emission spectrum. As there are often two such DAS components this has led to the conclusion of two distinct trapping kinetics, which occur roughly in the 40–60 and 80–130 ps time range. In order to explain these results it has been suggested that the 40–60 component may be associated with trapping from the core and the longer decay with trapping from the LHCI complexes of the external antenna. On the other hand, it was initially shown [14], and subsequently confirmed [18], that the effective trapping time in maize PSI–LHCI, calculated from the DAS, varies significantly as a function of the emission wavelength, increasing in a monotonic fashion from 700 nm to 760 nm across the emission band. This demonstration suggests that the trapping dynamics require a somewhat more detailed explanation than that previously suggested, based on the analysis of two "positive" DAS components only. Moreover, whereas these previous analyses [14,18] clearly demonstrate the wavelength dependence of the effective trapping times, they seem to have considerably underestimated the extent of this phenomenon. In order to clarify the situation we have re-examined the wavelength dependence of the trapping times in a preparation of PSI–LHCI prepared from maize by the solubilisation of thylakoid membranes using the mild detergent octyl-glucopyranoside (OGP) [6,14,18]. The results permit determination of

i) the intrinsic trapping time from the directly excited bulk.
ii) the large effective trapping time variation, as a function of wavelength, associated with the low energy chlorophylls in the wavelength range 700–760 nm
iii) the overall PSI–LHCI effective trapping time
iv) the marked contribution of excited state diffusion limitation to the effective photochemical trapping in PSI–LHCI.

Moreover they also

i) provide evidence that the red spectral states are not quenching states.
ii) indicate the presence in PSI–LHCI of at least one spectral form which emits at lower energy than the F735 form.

These conclusions are reached directly from the experimental data, without the need to use the usual compartmental type modelling, on which there is still significant debate in the literature.

## 2. Materials and methods

PSI–LHCI and LHCI were prepared by the method of Croce et al. [6,10] which employs the mild detergent OGP to solubilise the thylakoid membranes. Steady-state fluorescence emission spectra were measured at 90° with respect to the excitation beam using a CCD camera (Princeton, Applied Physics) as a detector, with a spectral resolution of 0.25 nm and were corrected for the instrument wavelength sensitivity. The excitation beam was provided by a xenon lamp passed through a Jasco monochromator with the transmittance half-width adjusted to either 1 or 2 nm, depending on the excitation wavelength. The emission spectra were measured across a Schott (Wayzata, MN) OG 530 filter. When excitation was into the $Q_y$ absorption band, the emission spectrum was corrected for the stray excitation "spike" by means of measurements performed either on the same sample, but after complete fluorescence quenching by addition of DBMIB (2,5-Dibromo-6-methyl-3-isopropyl-1,4-benzoquinone, 80 mM), or on a scattering suspension of glycogen. In this way it was possible to completely eliminate the scattering spike to within ±5 nm of the spike maximum for all excitation wavelengths.

Time-resolved fluorescence measurements with picosecond resolution were performed using the time-correlated single-photon counting (TCSPC) technique, as previously described [18]. In brief, the excitation source was a pulsed diode laser (PicoQuant GmbH, Berlin, Germany), controlled by a PicoQuant PDL 800-B unit, peaking at 632 nm and operating at a repetition rate of 20 MHz. The emission were passed through a monochromator (Jasco CT-10, Tokyo, Japan) and detected by a cooled microchannel plate photomultiplier tube (Hamamatsu R3809U-51, Hamamatsu, Japan). The instrument response function was measured using the reference dye DCI′, as previously described [19], resulting in an overall response of about 80 ps (FWHM) which after deconvolution yielded a time resolution of 10–20 ps. The emission decays were recorded at 10 nm intervals between 680 and 760, corrected for instrument wavelength sensitivity, and analysed globally by means of an algorithm developed in the laboratory [19].

The effective trapping time for antenna excited states, as a function of the detection wavelength, was determined from the decay associated spectra (DAS), by calculating the average lifetime which is defined as $\tau_{av}(\lambda) = \left(\sum_i A_i(\lambda)\cdot\tau_i\right)/\sum_i A_i(\lambda)\right)$. As previously described [14] this parameter has been demonstrated to be the effective trapping time. It is worth noting that the interpretation of the physical meaning of $\tau_{av}(\lambda)$ is independent of the details of the primary photochemical reactions, which are still a matter of debate.

The spectral overlap integral (SOI) for a bulk chlorophyll, acting as donor, and a red chl form, acting as acceptor, in a native protein environment was approximated on the basis of the calculated absorption spectrum both for weak (bulk pigment, S = 0.8) and strong coupling (red form, S = 4) to a phonon bath of mean frequency $\nu_m = 20\ cm^{-1}$, as previously described [20]. In short, we have used the set of vibrational frequencies and Franck–Condon factors reported in hole burning studies by Gillie et al. [21] as the input data for a Fast Fourier Transform algorithm used to numerically estimate the normalised chlorophyll a bandshape. The normalised fluorescence spectrum was obtained by the mirror image of the absorption bandshape and the Stokes shift determined by the Stepanov relation [20]. When a donor molecule, D, having the absorption maximum at $\nu_0^D$ and florescence spectrum $F(\nu_0^D,\nu)$, and an acceptor molecule, A, with absorption maximum at $\nu_0^A$ and absorption spectrum $\varepsilon(\nu_0^A,\nu)$ are considered, the SOI was determined by:

$$SOI\left(\nu_0^A-\nu_0^D\right) = \int_0^\infty d\nu\,\nu^{-4}F\left(\nu_0^D,\nu\right)\varepsilon\left(\nu_0^A,\nu\right), \quad (1)$$

as a function of the energy difference between the acceptor absorption maximum and the donor absorption maximum $\Delta E = \nu_0^A-\nu_0^B$.

## 3. Results and discussion

### 3.1. Fluorescence decay analysis of maize PSI–LHCI

The excited state trapping kinetics were studied in a PSI–LHCI supercomplex isolated from *Zea mais* and purified as described by Croce et al. [6,10]. Fluorescence decay, recorded in the 680–760 nm interval, are described in a global fit analysis, by three dominant components characterized by lifetimes of 13 ± 2 ps, 41 ± 5 ps and 74 ± 6 ps, and a minor component with an associated lifetime of 785 ± 30 ps. The confidence limits are the standard deviation of the fit parameters obtained from five independent measurements made on the same preparation. In our experience, the global fit minimum is rather broad, in agreement with others [22], and the standard deviations for measurements made on the same sample are an indication of this. The present results are very similar and within the experimental uncertainties of the solutions previously obtained by Engelmann et al. [18] for the same type of preparation, and using the same experimental set-up. Therefore, we have decided to average the results reported in ref. [18], with those obtained in the new PSI–LHCI preparation in order to extend the statistics. It is these averaged results which will be analysed in the present study. In most

fluorescence decay experiments of the kind presented here the errors distribution is not given. Typically, only the results of single decay measurements are presented and the confidence bounds are those associated with the fit of a particular measurement, which is then used for compartmental modelling.

In a study of this kind it is usual to present the decay associated spectra (DAS). These spectra are represented as the amplitude of each decay component as a function of the wavelength and are presented here as an inset (Fig. 1). The data are also shown in a modified version of the conventional DAS where the amplitude is replaced by the fluorescence yield ($A_i(\lambda) \cdot \tau_i$) versus wavelength. Each of these spectra represents the contribution of a given lifetime ($\tau_i$) to the steady-state emission spectrum. The main reason for this departure from the conventional representation is to clearly show the spectral characteristics of a low amplitude component with an ~800 ps lifetime which, despite its very low amplitude, contributes significantly to the steady state fluorescence by virtue of its relative long lifetime. Even when the fit results are presented in terms of yield, rather than the common representation in terms of DAS, it is apparent that three decay components (mean values for the two preparation batches of 12 ± 2 ps, 33 ± 3 ps and 77 ± 4 ps) are dominant. This is in broad agreement with measurements made by others [23,24], though there are differences with respect to Ihalainen et al. [17] and Slavov et al. [15], who seemed to have used preparations with a low red form content, as judged by the steady state spectra presented.

With our resolution the fastest decay detected in this preparation is around 12 ± 2 ps. This decay displays a small negative component at wavelengths above 700 nm and thus could describe a mixed decay, most of which is expected to be due to photochemical trapping (positive values) with a possible small bulk-to-red form energy transfer represented by the negative values. However, the minor negative values are all well inside the 2σ error range and thus are not significantly different from the zero line. Thus, it is reasonable to consider the 12 ps component as substantially a decay component. A similar component, with little or no negative amplitude, is commonly encountered in the 11–20 ps interval for different PSI–LHCI preparations [17,18,22,23,25]. Bulk to red form transfer components are best observed in Streak Camera measurements, which have a better time resolution than TCSPC. Ihalainen et al. [17] have resolved a ~5 ps component with approximately conservative positive and negative structures, as is expected for a pure transfer component.

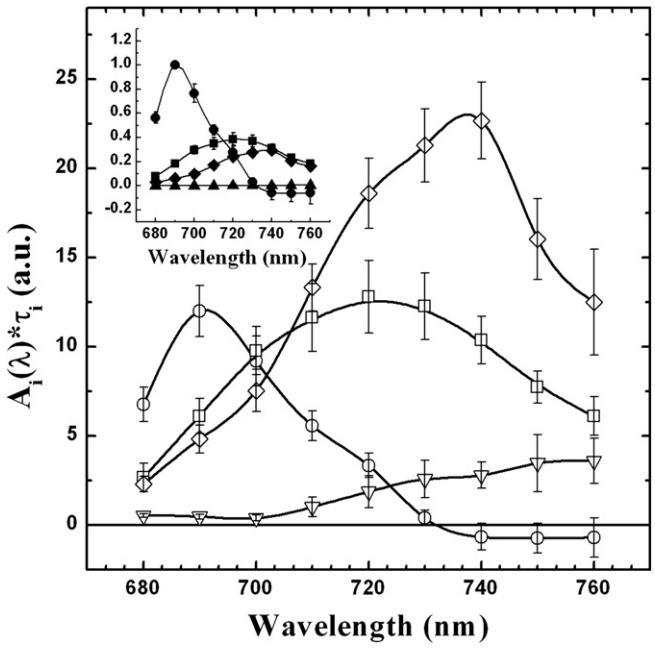


**Fig. 1.** Analysis of the fluorescence decay in PSI–LHCI. Inset: decay associated spectra; circles: 12 ± 2 ps; squares: 33 ± 3 ps; diamonds: 77 ± 4 ps; triangles: 787 ± 30 ps. Main panel: contribution of each decay component to the fluorescence yield ($A_i(\lambda) \cdot \tau_i$), as a function of the emission wavelength; contribution associated with the 12 ± 2 ps (circles); 33 ± 3 ps (squares); 77 ± 4 ps (diamonds); 787 ± 30 ps (triangles). The DAS values and the lifetimes are the weighted mean, obtained from two independent purifications of PSI–LHCI, each of which was measured five times. The error bars of the DAS are the standard deviation of the weighted mean and those of $A_i(\lambda) \cdot \tau_i$ are the propagated confidence levels.

While the 12 ps decay displays little or no yield (or amplitude) above 710 nm, the 33 ± 3 ps and 77 ± 4 ps decays display maxima at or above 720 nm and cover all the low energy spectral interval. Thus the energy levels present in the 12 ps component are those characteristic of the bulk antenna chlorophylls while there are pronounced contributions from the low energy states (red forms) in the 33 and 77 ps decays.

The fourth component, which is very long-lived (787 ± 30 ps) and has extremely low amplitudes but significant yield, is also present, as previously described [18,23,25]. A similar low amplitude component in PSI–LHCI form Arabidopsis, with a decay time of 230 ps was recently noticed [22]. Long-lived decays of low amplitude are usually considered to be associated with uncoupled chlorophylls formed during complex preparation. However, uncoupled chlorophylls emit in the blue of the $Q_y$ transition interval, usually around 670 nm. In the case of the 800 ps decay, however, the emission is markedly red shifted (Fig. 1). Thus, it could represent a fraction of complexes in which energy transfer from the low energy states, and hence trapping, is very slow, possibly, but not necessarily, due to the preparation procedure. As we feel that this component should not be ignored, our analyses will usually be performed both in its presence and absence.

### 3.2. Wavelength dependence of the effective photochemical trapping time

Fig. 2 shows the steady state emission spectrum ($F(\lambda) \equiv \sum A_i(\lambda) \cdot \tau_i$) calculated from the DAS, considering (Fig. 2B), or ignoring (Fig. 2A), the 800 ps component. It is clear that the impact of the ~800 ps component increases with increasing wavelength and at 760 nm it appears to account for about 20% of the steady state emission, on the basis of the mean values. The reconstructed steady state spectra are in close agreement with the measured steady state emission spectrum for this same preparation (not shown) and with those presented by Croce et al. [6,24] for PSI–LHCI purified according to the same preparation method. It was estimated that about 80% of the excited states populate the low energy forms in the steady state [6]. This, however, is not the case for the PSI–LHCI prepared from Arabidopsis [15–17,25], where very substantial differences may be noted (see below).

Fig. 2 also shows the calculated effective trapping time as a function of wavelength, ($\tau_{av}(\lambda)$), which is calculated from the DAS as described in Materials and methods section. It is seen that the fastest trapping occurs from chlorophylls emitting in the 680–690 nm interval (~18 ps), wavelengths which are characteristic of the bulk antenna emission. At emission wavelengths beyond 700 nm, associated with excited state population of the low energy forms, the value of $\tau_{av}(\lambda)$ increases dramatically to 70 or 85 ps, according to whether the 800 ps component is included. We have calculated the value $\tau_{av}(\lambda)$ for a number of published experiments performed with PSI–LHCI prepared from Arabidopsis. Though the preparations display considerable variability, particularly in red form content (see below), the large increases in $\tau_{av}(\lambda)$ across the long wavelength emission band are always present, with maximal values which range from 65 ps [25], 73 ps [15], 92 ps [16] and 130 ps [17]. The present value of $\tau_{av}(\lambda)$~18 ps for the 680–690 nm spectral region is in very close agreement with the measured effective trapping time of 17 ± 5 ps for the isolated core complex from maize [18]. It is also in close agreement with values obtained by target modelling analytical approaches performed by other laboratories [16,22] for PSI–LHCI from

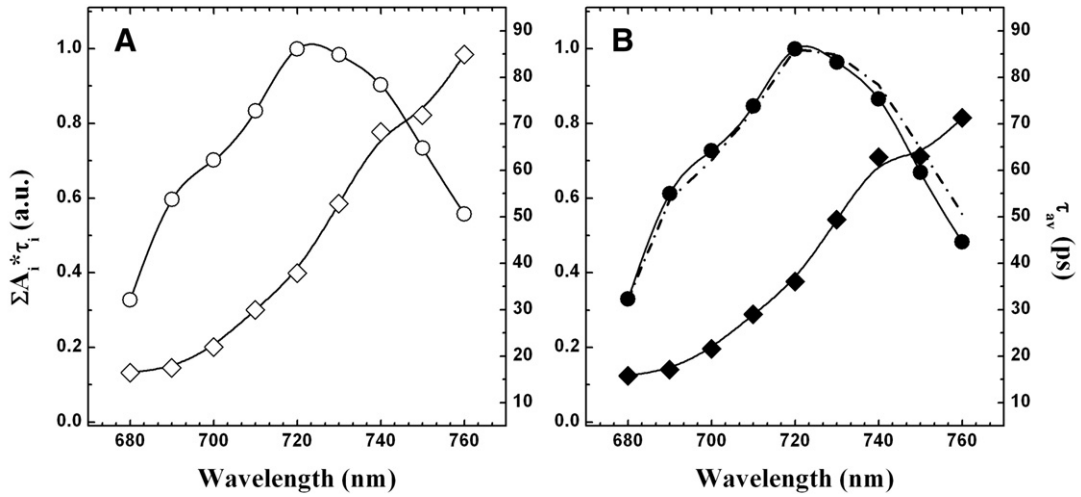


**Fig. 2.** Reconstruction of the steady-state emission spectra from the DAS (circles) and the wavelength dependence of the $\tau_{av}$ parameter (diamonds), computed using all of the lifetimes retrieved from the global analysis (Panel A, open symbols) or neglecting the long-lived 787 ± 30 ps component (Panel B, solid symbols). In Panel B is also shown the reconstructed steady-state spectrum of Panel A (dash-dotted line) to facilitate comparison.

Arabidopsis (~18 ps). Thus, the present $\tau_{av}(\lambda)$~18 ps in the 680–690 nm interval is interpreted as the effective photochemical trapping time of the core. We add that the high energy LHCI pigments are also expected to emit in the same spectral interval, which could complicate our simple interpretation concerning the "effective photochemical trapping time of the core". However, we expect their contribution to the 18 ps average lifetime to be minor as these pigments, which are very closely associated with the low energy pigments (red forms), will probably be substantially quenched. This is the case for isolated, or reconstituted, LHCI complexes where only minor steady state emission is measured from the high energy pigments. If this should not be the case, and the LHCI high energy pigments make a (small) contribution to average lifetime in the 680–700 nm emission wavelength interval, then the present value of 18 ps time would be an overestimate of the core trapping time. However, we underline, that our interpretation is in agreement with the measurements on the isolated PSI core from maize, measured with the same instrument [18].

In the same way the large and progressive increases in $\tau_{av}(\lambda)$ associated with the red forms also represent the effective trapping time from the low energy antenna states emitting at these wavelengths. While, in principal, many different rate processes may contribute to $\tau_{av}(\lambda)$, in the present case the wavelength dependence must be due only to those involving the transfer of energy from the bulk to the low energy states and the reverse process. All other processes will be independent of wavelength over the long wavelength emission band. The present data do not permit us to directly distinguish between inward and outward energy flow between the red forms and the bulk antenna. However, we tend to exclude a significant influence of bulk antenna to red form energy transfer processes on the marked $\tau_{av}(\lambda)$ heterogeneity. This is because the spectral overlap integral (SOI), involved in both the Förster and the Dexter transfer mechanisms, when expressed as a function of the donor (fluorescence)/acceptor (absorption) energy separation (ΔE), is markedly asymmetrical (Fig. 3). For energy flow from a low energy donor to a higher energy acceptor the SOI declines steeply with increasing ΔE. This is shown in Fig. 3, where the overlap integral has been calculated for energy transfer between a bulk antenna chlorophyll ($S = 0.8$, $\nu_m = 20\ cm^{-1}$) and a red form ($S = 4$, $\nu_m = 20\ cm^{-1}$). See Materials and methods section for details of the calculations. On the other hand, for energy transfer from a high energy donor to a lower energy acceptor there is an initially steep decline of SOI over a ΔE of about 500 $cm^{-1}$ which then assumes a roughly constant value up to about 1500 $cm^{-1}$ due to the vibronic bands. Previously, qualitatively similar results were found for chlorophyll in solution [26]. The wavenumber spread in Fig. 2 is approximately 1500 $cm^{-1}$. Thus, energy transfer into the red forms is not expected to be particularly wavelength dependent over the 700–760 nm interval (1100 $cm^{-1}$). On the other hand the SOI for "uphill" energy transfer is markedly dependent on ΔE and presumably is the basis for the $\tau_{av}(\lambda)$ heterogeneity. Of course, the transfer time between any one donor/acceptor pair is not wavelength dependent. Thus, we interpret the $\tau_{av}(\lambda)$ heterogeneity as being due to the spectral overlap of different low energy spectral states i.e. the wavelength dependent heterogeneous $\tau_{av}(\lambda)$ values indicate the transfer rate from a combination of different red forms which changes with the wavelength.

Despite the pronounced wavelength dependency of the effective trapping, these data may be used to calculate the overall effective trapping time for the whole of PSI–LHCI. This can be achieved by weighting the effective trapping $\tau_{av}(\lambda)$ for the excited state

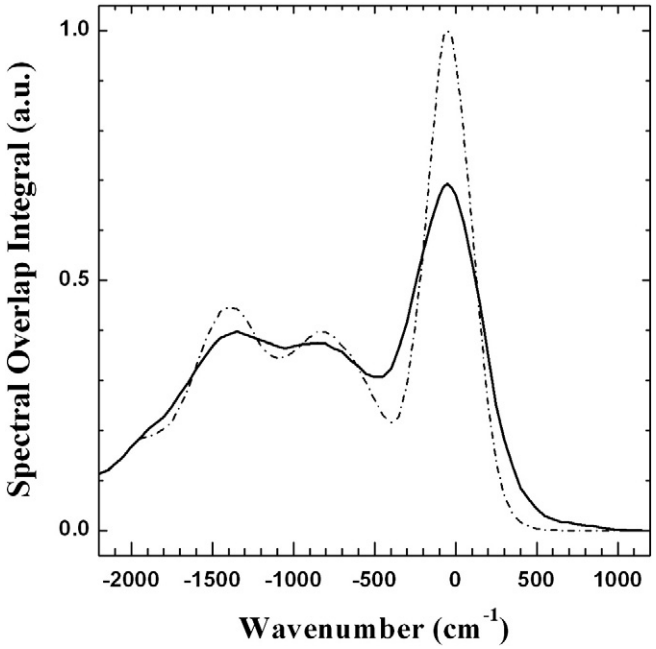


**Fig. 3.** Spectral overlap integral (SOI) for energy transfer between a bulk antenna chlorophyll ($S = 0.8$, $\nu_m = 20\ cm^{-1}$; dash-dotted line) and a red form ($S = 4$, $\nu_m = 20\ cm^{-1}$; solid line) calculated as described in Eq. (1).

population probability ($p(\lambda)$) at each detection wavelength. The excited state probability, $p(\lambda)$, is given by the calculated steady state emission spectrum (Fig. 2), under the normalization condition $\sum_{\lambda} p(\lambda) \equiv 1$. Thus, the overall trapping time, $\tilde{\tau}_{av}$, is defined as $\tilde{\tau}_{av} = \sum_{\lambda} \tau_{av}(\lambda) \cdot p(\lambda)$. In this way we determine the overall trapping time for maize PSI–LHCI as 40 ps, i.e. approximately 2.1 times that of the core trapping time (18 ps). This factor is very similar to the value of 2.4 recently determined [22], using a different approach. Thus, two different approaches lead to essentially the same result which adds credibility to these numbers for PSI–LHCI. The result also underlines the marked diffusion limiting kinetic bottleneck associated with the "uphill" energy flow from the red forms to the core antenna and trapping. Thus, of the two higher plant Photosystems, PSI–LHCI would appear to have a greater contribution to the trapping kinetics by energy diffusion in the antenna, which accounts for slightly more than 50% of the overall trapping time. On the other hand, for PSII–LHCII the diffusion kinetic limitation has been estimated to be around 20–30% [27,28]. Yet, even in the presence of such a marked diffusion limitation component to the overall trapping, the quantum efficiency of PSI–LHCI is considerably greater than that of PSII–LHCII, with values exceeding 0.95 over the whole emission band.

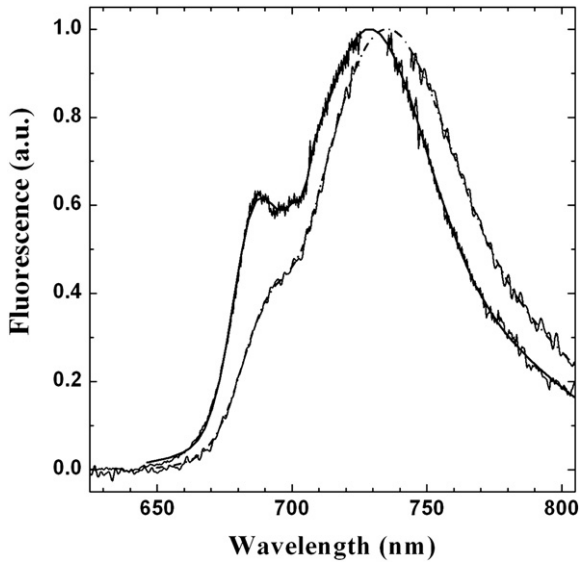


**Fig. 4.** Steady-state fluorescence emission spectra of LHCI (thick solid line) and PSI–LHCI (thin solid line) recorded upon direct excitation of red spectral forms at 735 nm.

### 3.3. Long-wavelength chlorophyll spectral forms in PSI–LHCI extending above 735 nm

Concerning Fig. 2, it is interesting to note that the $\tau_{av}(\lambda)$ values do not reach a plateau at wavelengths near and above 735 nm, as would be expected if the 735 nm emission state were the lowest energy form, as is often thought (e.g. [29–32]). In vitro reconstitution experiments suggest that both Lhca3 and Lhca4 bind this low energy state with a small difference (circa 2 nm) in the peak emission [12,22,31]. The fact that the $\tau_{av}(\lambda)$ values in intact PSI–LHCI, continue to increase in a significant manner beyond this wavelength range can be explained by the presence of at least another low energy form which emits beyond 735 nm. The emission band shape of the 735 emission state was earlier determined [33,34] and was shown to be extremely broad, presumably due to very strong electron phonon coupling, possibly associated with a charge transfer state [31]. Its low energy tail extends well above 770 nm. We therefore suggest that the data on $\tau_{av}(\lambda)$ heterogeneity in the longest wavelength interval investigated may be due to the emission overlap between the 735 emission state and a putative lower energy state(s). This conclusion is supported by the steady state emission spectra presented in Fig. 4 for the LHC I preparation and PSI–LHCI. The LHCI preparation contains approximately equal numbers of the Lhca1/4 and Lhca2/3 dimers which were recently shown to have very similar spectral properties [35]. The spectra presented in Fig. 4 were recorded with excitation directly in the emission band at 735 nm, in order to capture both the pre-equilibrium emission from the directly excited red state [33,34], as well as the equilibrated emission. The experiment was performed as described in [33,34]. The two spectra, LHCI and PSI–LHCI, are overlapped with normalisation at the emission maximum. Concerning the LHCI spectrum the estimated maximum is close to 730 nm and for PSI–LHCI it is near 735 nm. The equilibrium emission maxima are near 720 nm for LHCI and 730 nm for PSI–LHCI [33,34]. Thus, the PSI–LHCI emission is red shifted with respect to that of LHCI. Furthermore, it is evident that the PSI–LHCI spectrum is considerably broader in the long wavelength wing with respect to LHCI. The same conclusion is reached by comparing the reconstituted Lhca4 emission spectrum [36] with the present spectra (Fig. 4). In the earlier study [34] in which the long wavelength, pre-equilibration, emission spectrum was determined after direct excitation within the emission band itself, in both an LHCI preparation and PSI–LHCI, it was evident that the LHCI pre-equilibration fluorescence maximum at 735 nm remained constant with increasing excitation wavelength between 720 and 740 nm. On the other hand, for PSI–LHCI the pre-equilibrium emission maximum shifted to 745 nm when excitation was performed over the same wavelength interval. In addition, the low temperature time resolved data for PSI–LHCI [24,37] show a slowly decaying component that has an associated DAS peaking near 740 nm, the band-shape of which is strongly asymmetric towards longer wavelengths. It was suggested that the detergent based techniques used to detach the LHCI complexes, and which are also present in reconstitution experiments, may destroy this very low energy state(s). We also exclude any contribution by the small amounts of low energy states detected in the PSI core [6] as, in higher plants, their emission is at wavelengths well below 735 nm. Thus a number of independent experimental approaches point in the same direction and indicate the presence of lower energy states in intact maize PSI–LHCI than in the isolated maize LHCI itself. Presumably, these states are destroyed during the detachment of LHCI from intact PSI and they are apparently not formed during reconstitution.

### 3.4. Comparison with other higher plants PSI–LHCI preparations

Over the past decade a number of studies on higher plant PSI–LHCI have been performed on complexes isolated from Arabidopsis [15–17,25]. The time resolved fluorescence data [25] were measured and analysed in our laboratory and were thus performed with the same instrumental set up as the maize preparation discussed above. The considerable data variability for the Arabidopsis preparations renders it difficult to analyse and discuss these data in detail. This variability is exemplified by the steady state fluorescence emission wavelength ratio (720/690) nm, which is an approximate indicator of the ratio for bulk emission (690 nm) and the low energy emission (720 nm). The data have been calculated from the DAS presented in each paper. The values for the 720/690 ratio for the various Arabidopsis PSI–LHCI preparations vary between 0.5 and 1.25 [15–17,25] while that for the different maize preparations, including the present one, are close to 1.7. Thus in all cases the red form content for the Arabidopsis preparations seems to be lower than that of the maize preparations. These differences may well be due to the detergents employed. In the case of the maize preparations the detergent used was octyl-gluco-pyranoside (OGP) instead of the more commonly used dodecyl-maltoside (DM). OGP is known to lead to a lesser uncoupling of bulk chlorophylls than DM [37] and does not modify the band shape of the low energy fluorescence tail [6], a

characteristic of fundamental importance in studies of this kind. In the Arabidopsis preparations DM was employed.

We have calculated the $\tau_{av}(\lambda)$ for trapping from the bulk antenna (680–690 nm) in these preparations, which range from about 25 ps [15] to 35 ps [25] and 45 ps [17]. These values may indicate a slower photochemical trapping in Arabidopsis PSI–LHCI with respect to the maize photosystem, though given the rather broad data distribution this suggestion should be taken with caution.

As mentioned above, in the Arabidopsis studies, in all cases the $\tau_{av}(\lambda)$ values increase across the low energy emission band (>700 nm), as in maize. Thus while these data display the low energy kinetic bottleneck, indicative of pronounced diffusion limited trapping, as described for maize, it is not possible to draw any more detailed conclusions due to the data spread.

### 3.5. Physiological role of long wavelength spectral forms in PSI

The present paper underlies the significant variation $\tau_{av}(\lambda)$ across the emission band, which displays an almost linear increase as a function of the decrease in energy of the low energy spectral states. This point is relevant to the discussion on the physiological role of the low energy (red) forms. While it has been demonstrated that they increase the antenna cross section under "shade light" conditions [38] evidence was presented [17] that red forms associated with LHCI proteins have a low fluorescence yield, a suggestion which opened the possibility that they may be quenching states, possibly involved in photoprotection (e.g. [17]). Subsequently this claim has however been disputed [39] and the present data are also in disagreement with this. If the red states were, in fact, quenching states one would not expect them to display the highest $\tau_{av}(\lambda)$ of the intact photosystem, which steadily increases across the low energy emission band. That the red forms do not represent a quenched state was also demonstrated earlier [6,37]. In this respect, it might be interesting to notice that the carotenoid triplet state populated by triplet–triplet energy transfer from the red spectral form has been detected both in isolated LHCI [40], as well as the intact PSI supercomplex of thylakoids [41]. This would represent an efficient photoprotective strategy since carotenes appears to be specifically coupled to the spectral forms which carry most of the excited state population at steady state, and hence have the highest probability of populating the potentially harmful triplet state via intersystem crossing.

## References


[1] B.D. Bruce, R. Malkin, Subunit stoichiometry of the chloroplast photosystem I complex, J. Biol. Chem. 263 (1988) 7302–7308.
[2] A. Ben-Shem, F. Frolow, N. Nelson, Crystal structure of plant photosystem I, Nature 426 (2003) 630–635.
[3] R.C. Jennings, R. Bassi, G. Zucchelli, Antenna structure and energy transfer in higher plant photosystems, Top. Curr. Chem. 177 (1996) 147–181.
[4] E.J. Boekema, P.E. Jensen, E. Schlodder, J.F.L. van Breemen, H. van Roon, H.V. Scheller, J.P. Dekker, Green plant photosystem I binds light-harvesting complex I on one side of the complex, Biochemistry 40 (2001) 1029–1036.
[5] R. Croce, R. Bassi, The light-harvesting complex of photosystem I: pigment composition and stoichiometry, in: G. Garab (Ed.), Photosynthesis: Mechanisms and Effects, vol. 1, Kluwer Academic Publishers, Dordrecht, 1998, pp. 421–424.
[6] R. Croce, G. Zucchelli, F.M. Garlaschi, R. Bassi, R.C. Jennings, Excited state equilibration in the photosystem I light harvesting complex: P700 is almost isoenergetic with its antenna, Biochemistry 35 (1996) 8572–8579.
[7] E. Engelmann, T. Tagliabue, N.V. Karapetyan, F.M. Garlaschi, G. Zucchelli, R.C. Jennings, (2001) CD spectroscopy provides evidence for excitonic interactions involving red-shifted chlorophyll forms in photosystem I, FEBS Lett. 499 (2001) 112–115.
[8] T. Morosinotto, S. Castelletti, J. Breton, R. Bassi, R. Croce, Mutation analysis of Lhca1 antenna complex. Low energy absorption forms originate from pigment–pigment interactions, J. Biol. Chem. 277 (2002) 36253–36261.
[9] M. Mozzo, T. Morosinotto, R. Bassi, R. Croce, Probing the structure of Lhca3 by mutation analysis, Biochim. Biophys. Acta Bioenerg. 1757 (2006) 1607–1613.
[10] R. Croce, G. Zucchelli, F.M. Garlaschi, R.C. Jennings, A thermal broadening study of antenna chlorophylls in PSI-200, LHCI, and PSI core, Biochemistry 37 (1998) 17355–17360.
[11] R. Croce, T. Morosinotto, S. Castelletti, J. Breton, R. Bassi, The Lhca antenna complexes of higher plant photosystem I, Biochim. Biophys. Acta Bioenerg. 1556 (2002) 29–40.
[12] V.H.R. Schmid, K.V. Cammarata, B.U. Bruns, G.W. Schmidt, *In vitro* reconstitution of the photosystem I light-harvesting complex LHCI-730: heterodimerization is required for antenna pigment organization, Proc. Natl. Acad. Sci. U.S.A. 94 (1997) 7667–7672.
[13] B. Gobets, R. van Grondelle, Energy transfer and trapping in photosystem I, Biochim. Biophys. Acta Bioenerg. 1507 (2001) 80–99.
[14] R.C. Jennings, G. Zucchelli, R. Croce, F.M. Garlaschi, The photochemical trapping rate from red spectral states in PSI–LHCI is determined by thermal activation of energy transfer to bulk chlorophylls, Biochim. Biophys. Acta Bioenerg. 1557 (2003) 91–98.
[15] C. Slavov, M. Ballottari, T. Morosinotto, R. Bassi, A.R. Holzwarth, Trap limited charge separation kinetics in higher plant photosystem I complexes, Biophys. J. 94 (2008) 3601–3612.
[16] J.A. Ihalainen, P.E. Jensen, A. Haldrup, I.H.M. van Stokkum, R. van Grondelle, H.V. Scheller, J.P. Dekker, Pigment organization and energy transfer dynamics in isolated photosystem I (PSI) complexes from Arabidopsis thaliana depleted of the PSI-G, PSI-K, PSI-L, or PSI-N subunit, Biophys. J. 83 (2002) 2190–2201.
[17] J.A. Ihalainen, R. Croce, T. Morosinotto, I.H.M. van Stokkum, R. Bassi, J.P. Dekker, R. van Grondelle, Excitation decay pathways of Lhca proteins. a time resolved fluorescence study, J. Phys. Chem. B 109 (2005) 21150–211158.
[18] E. Engelmann, G. Zucchelli, A.P. Casazza, D. Brogioli, F.M. Garlaschi, R.C. Jennings, Influence of photosystem I — light harvesting complex I antenna domains on fluorescence decay, Biochemistry 45 (2006) 6947–6955.
[19] G. Tumino, A.P. Casazza, E. Engelmann, F.M. Garlaschi, G. Zucchelli, R.C. Jennings, Fluorescence lifetime spectrum of the PSII core complex: photochemistry does not induce specific reaction centre quenching, Biochemistry 47 (2008) 10449–10457.
[20] G. Zucchelli, R.C. Jennings, F.M. Garlaschi, G. Cinque, R. Bassi, O. Cremonesi, The calculated in vitro and in vivo chlorophyll a absorption band shape, Biophys. J. 82 (2002) 378–390.
[21] J.K. Gillie, G.J. Small, J.H. Golbeck, Nonphotochemical hole burning of the native antenna complex of photosystem I (PSI-200), J. Phys. Chem. 93 (1989) 1620–1627.
[22] E. Wientjes, I.H.M. van Stokkum, H. van Amerongen, R. Croce, The role of the individual Lhcas in Photosystem I excitation energy trapping, Biophys. J. 101 (2011) 745–754.
[23] B. van Oort, A. Amunts, J.W. Borst, A. van Hoek, N. Nelson, H. van Amerongen, R. Croce, Picosecond fluorescence of intact and dissolved PSI–LHCI crystals, Biophys. J. 95 (2008) 5851–5861.
[24] R. Croce, D. Dorra, A.R. Holzwarth, R.C. Jennings, Fluorescence decay and spectral evolution in intact photosystem I of higher plants, Biochemistry 39 (2000) 6341–6348.
[25] P. Galka, S. Santabarbara, T.T. Khuong, H. Degand, P. Morsomme, R.C. Jennings, E.J. Boekema, S. Caffarri, Functional analysis of the plant photosystem I—light harvesting complex II supercomplex reveal that light harvesting complex II loosely bound to photosystem II is a very efficient antenna for photosystem I in state II, Plant Cell 24 (2012) 2963–2978.
[26] L.L. Shipman, D.L. Housman, Föerster transfer rates for chlorophyll a, Photochem. Photobiol. 29 (1979) 1163–1167.
[27] R.C. Jennings, G. Elli, F.M. Garlaschi, S. Santabarbara, G. Zucchelli, Selective quenching of the fluorescence of core chlorophyll–protein complexes by photochemistry indicates that photosystem II is partly diffusion limited, Photosynth. Res. 66 (2000) 225–233.
[28] K. Broess, G. Trinkunas, A. van Hoek, R. Croce, H. van Amerongen, Determination and excitation migration time in photosystem II — consequences for the membrane organisation and charge separation parameters, Biochim. Biophys. Acta 1777 (2008) 404–409.
[29] T. Morosinotto, J. Breton, R. Bassi, R. Croce, The nature of a chlorophyll ligand in Lhca proteins determines the far red fluorescence emission typical of photosystem I, J. Biol. Chem. 278 (2003) 49223–49229.
[30] F. Passarini, E. Wientjes, H. van Amerongen, R. Croce, Photosystem I light harvesting complex Lhca4 adopts multiple conformations: red forms and excited-state quenching are mutually exclusive, Biochim. Biophys. Acta Bioenerg. 1797 (2010) 501–508.
[31] R. Croce, A. Chojnicka, T. Morosinotto, J.A. Ihalainen, F. van Mourik, J.P. Dekker, R. Bassi, R. van Grondelle, The low energy forms of photosystem I light harvesting complexes: spectroscopic properties and pigment–pigment interaction characteristics, Biophys. J. 93 (2007) 2418–2428.
[32] E. Romero, M. Mozzo, I.H.M. van Stokkum, J.P. Dekker, R. van Grondelle, R. Croce, The origin of the low energy form of photosystem I complex Lhca4: mixing of the lowest exciton with a charge transfer state, Biophys. J. 96 (2009) L35–L37.
[33] R.C. Jennings, F.M. Garlaschi, E. Engelmann, G. Zucchelli, The room temperature emission band shape of the lowest energy spectral form in LHCI, FEBS Lett. 547 (2003) 107–110.
[34] R.C. Jennings, G. Zucchelli, E. Engelmann, F.M. Garlaschi, The long wavelength chlorophyll states of plant LHCI at room temperature: a comparison with PSI–LHCII, Biophys. J. 87 (2004) 488–497.
[35] E. Wientjes, R. Croce, The light harvesting complexes of higher plant photosystem I: Lhca1/4 and Lhca2/3 form two red emitting heterodimers, Biochem. J. 433 (2011) 477–485.
[36] G. Zucchelli, T. Morosinotto, F.M. Garlaschi, R.C. Jennings, The low energy emitting states of the Lhc4 subunit of higher plant photosystem I, FEBS Lett. 579 (2005) 2071–2076.
[37] R. Croce, (1997) Doctoral thesis, University of Milano.

[38] A. Rivadossi, G. Zucchelli, F.M. Garlaschi, R.C. Jennings, The importance of PSI chlorophyll red forms in light harvesting by leaves, Photosynth. Res. 60 (1999) 209–215.
[39] E. Wientjes, I.H.M. van Stokkum, H. van Amerongen, R. Croce, Excitation-energy transfer dynamics of higher plant photosystem I light harvesting complexes, Biophys. J. 100 (2011) 1372–1380.
[40] D. Carbonera, A. Agostini, T. Morosinotto, R. Bassi, Quenching of chlorophyll triplet states by carotenoids in reconstituted Lhca4 subunit of peripheral light–harvesting complex of photosystem I, Biochemistry 44 (2005) 8337–8346.
[41] S. Santabarbara, D. Carbonera, Carotenoid triplet states associated with the long-wavelength-emitting chlorophyll forms of photosystem I in isolated thylakoid membranes, J. Phys. Chem. B 109 (2005) 986–991.